Direct conversion of human fibroblasts to dopaminergic neurons

Ulrich Pfisterer[1], Agnete Kirkeby[1], Olof Torper[1], James Wood, Jenny Nelander, Audrey Dufour, Anders Björklund, Olle Lindvall, Johan Jakobsson, and Malin Parmar[2]

Departments of Experimental Medical Science and Clinical Sciences, Wallenberg Neuroscience Center, and Lund Stem Cell Center, Lund University, SE-221 84 Lund, Sweden

Edited* by Fred H. Gage, The Salk Institute, San Diego, CA, and approved May 13, 2011 (received for review March 31, 2011)

Recent reports demonstrate that somatic mouse cells can be directly converted to other mature cell types by using combined expression of defined factors. Here we show that the same strategy can be applied to human embryonic and postnatal fibroblasts. By overexpression of the transcription factors Ascl1, Brn2, and Myt1l, human fibroblasts were efficiently converted to functional neurons. We also demonstrate that the converted neurons can be directed toward distinct functional neurotransmitter phenotypes when the appropriate transcriptional cues are provided together with the three conversion factors. By combining expression of the three conversion factors with expression of two genes involved in dopamine neuron generation, *Lmx1a* and *FoxA2*, we could direct the phenotype of the converted cells toward dopaminergic neurons. Such subtype-specific induced neurons derived from human somatic cells could be valuable for disease modeling and cell replacement therapy.

Cellular reprogramming, the process by which somatic cells can be converted into induced pluripotent stem (iPS) cells and subsequently differentiated to mature cells, including specific types of neurons, has opened up new possibilities for disease modeling and cellular repair (1–5). Recently, it was shown that somatic cells can also be directly converted to other mature cell types by expression of a specific combinations of genes (6–9). Expression of Ascl1, Brn2, and Myt1l efficiently converted mouse embryonic fibroblasts (MEFs) and postnatal fibroblasts into functional neurons (induced neurons, or iN cells) (10). Cells generated via direct conversion do not pass through a pluripotent state, are probably not tumorigenic, and may serve as an interesting alternative to iPS cells for generating patient- and/or disease-specific neurons.

Here, we show the direct conversion of human fibroblasts into functional neurons using the same combination of neural conversion factors used for iN conversion of mouse fibroblasts (10). We also demonstrate that the expression of additional transcription factors leads to the generation of cells with properties of dopaminergic neurons, which is the cell type lost in Parkinson's disease. Our findings provide proof of principle that specific subtypes of iN cells can be produced from human somatic cells by transcription factor-mediated fate instruction combined with the three neural conversion factors.

Results

To investigate whether direct conversion into neurons from human somatic cells is possible, we established fibroblast cultures from human embryos aged 5.5–7 wk postconception (for details see Table S1). The head, the dorsal part of the embryo containing the spinal cord, and all red organs were removed, and the remaining tissue was dissociated and plated under standard fibroblast conditions (Fig. 1*A*). After one passage followed by a freeze–thaw cycle, the fibroblast identity and the absence of the neural crest marker *SOX10* in the resulting cell lines were confirmed (Fig. 1*B*, Figs. S1 and S2, and Tables S2 and S3). The cells were then used for conversion by delivering lentiviral vectors coding for Ascl1, Brn2, and Myt1l, the three factors previously identified as efficiently converting MEFs to neurons (10). Expression of the conversion factors in human embryonic fibroblasts (hEFs) was verified with quantitative RT-PCR (qRT-PCR) (Fig. S2 *A–C*). In cultures transduced with conversion factors and subsequently grown in N3 neural induction medium (11), cells with elongated neuron-like morphology became visible after 3–4 d (Fig. S2*D*). By 12 d after transduction, many cells exhibiting characteristic neuronal morphology and expressing βIII-tubulin could be detected (Fig. 2*A*). In parallel control cultures containing hEFs not infected with conversion factors but otherwise treated identically, neurons were never observed (Fig. 2*A*). The morphology of the human-derived iN (hiN) cells matured over time, and the vast majority of them had an elaborate neuronal morphology by day 24 (Fig. 2*A*). The efficiency of hiN generation was determined by using fibroblasts (passage 2) from three different embryos. We found that the number of hiN cells increased with time in culture. By day 24, on average, 1,600 neurons per cm^2 were present, corresponding to a conversion efficiency of 16% ± 4.3% (Fig. 2*B*). The capacity to form hiN cells decreased with one additional passage (from 9.0% to 4.53%, day 12) but then remained constant until passage 8 when the cells ceased to proliferate (Fig. 2*C* and Fig. S2 *E* and *F*).

More than 95% of the converted neurons expressed the neuron-specific cytoskeletal protein MAP2, which is enriched in dendrites (Fig. 2*D*). The great majority (≥90%) of the hiN cells also expressed synaptophysin, indicating the presence of synapses on the hiN cells (Fig. 2*E*). At 23 d after conversion, patch–clamp recordings showed that the resting membrane potential was approximately −34 mV and that depolarizing current injection did not induce action potentials, suggesting immaturity of the cells. However, at 30–32 d after transduction, the average resting membrane potential was approximately −59 mV (range: −30 mV to −78 mV), and the cells now exhibited electrophysiological properties of functional neurons (Table S4). Depolarizing current injection induced action potentials in ∼90% of recorded cells (Fig. 2*F*). In voltage–clamp mode, step depolarization induced fast-inactivating inward and outward currents characteristic of sodium and delayed-rectifier potassium currents, respectively (Fig. 2*G*). Action potentials and inward sodium currents were blocked by TTX (Fig. 2 *F* and *G*, *Right*). Biocytin labeling confirmed the neuronal morphology of recorded cells (Fig. S2*H*).

The expression of the three transgenes used for iN conversion was regulated by doxycycline, which must be supplied in the media throughout the culture period to maintain transgene expression (Fig. S2 *A–C*). To test whether continuous expression of the conversion factors is necessary for efficient hiN generation, we removed doxycycline at day 0 (i.e., never activated the transgenes), day 3, or day 7 after transduction. Doxycycline removal at day 0 resulted in only sporadic hiN formation, most likely because of nonspecific leakage of transgene expression, whereas withdrawal at day 3 or day 7 did not significantly change the number of neurons formed, the process length, or the number of projections (Fig. 3 *A* and *B*). These data suggest that conversion of fibroblasts into neurons using *Ascl1*, *Brn2*, and

Author contributions: O.L., J.J., and M.P. designed research; U.P., A.K., O.T., J.W., J.N., and A.D. performed research; U.P., A.K., O.T., J.W., A.B., O.L., J.J., and M.P. analyzed data; and M.P. wrote the paper.

The authors declare no conflict of interest.

*This Direct Submission article had a prearranged editor.

Freely available online through the PNAS open access option.

[1]U.P., A.K., and O.T. contributed equally to this work.

[2]To whom correspondence should be addressed. E-mail: malin.parmar@med.lu.se.

This article contains supporting information online at www.pnas.org/lookup/suppl/doi:10.1073/pnas.1105135108/-/DCSupplemental.

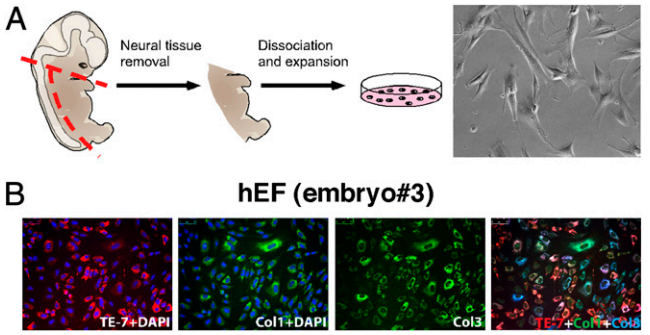

Fig. 1. Establishment of hEF cultures. (*A*) Fibroblasts isolated from human embryos were dissociated and plated under standard fibroblast conditions. The fibroblasts were passaged once, frozen, and subsequently used for experiments. (*B*) Immunostaining confirmed that the resulting cultures were composed of cells expressing collagen I and III, confirming their fibroblast identity, and TE-7 confirmed their mesodermal origin.

Myt1l only requires a pulse of transgene expression during the initiation of the conversion phase, after which the hiN cells mature into neurons without exogenous gene expression.

To determine the contribution of each conversion factor to the generation of hiN cells, we performed conversions using each of the three factors individually or pairwise. Although Ascl1 alone was sufficient to induce a neuron-like phenotype, including expression of MAP2 and βIII-tubulin without significant reduction in conversion efficiency, neither Brn2a nor Myt1l alone resulted in the formation of a substantial number of hiN cells (Fig. 3 *C* and *D*). However, the Ascl1-alone cells had a markedly different morphology with shorter processes than those observed for the cells converted with the three factors Ascl1, Brn2, and Myt1l (Fig. 3*C*). When combining the factors into pairs, we found that Ascl1 + Brn2 and Myt1l + Brn2 produced mature-looking neurons, whereas Ascl1 + Myt1l resulted in cells with less pronounced neuronal morphology (Fig. 3*C*). Thus, based on number of cells and morphological criteria, Ascl1 + Brn2 may be as efficient as Ascl1, Brn2, and Myt1l in generating hiN cells. However, electrophysiological recordings showed that cells converted with Ascl1 + Brn2, in contrast to the cells converted with Ascl1, Brn2, and Myt1l, did not exhibit the electrophysiological properties of mature neurons (resting membrane potentials between −20 mV and −75 mV; input resistances between 50 MΩ and 2 GΩ; $n = 12$) and thus are not converted neurons. These findings demonstrate that all three factors contribute to the conversion of human fibroblasts into functional neurons.

To exclude the possibility that contaminating neural progenitors, glia, or neural crest cells served as the cellular origin of the iN cells, we performed extensive immunocytochemical characterization and PCR analysis of the starting fibroblast cultures as well as fibroblasts cultured in N3 medium and doxycycline for 6 and 12 d. With the exception of very few neural crest cells detected in low-passage hEF cultures (<0.1% at passage 2), none of the other markers could be detected (Figs. S2*G* and S3 *A*–*H* and Tables S2 and S3). To completely rule out the possibility that hiN cells are neural crest derivatives, we next used a commercially available, long-term expanded human fetal lung fibroblast cell line (HFL1) (12), which is a homogenous fibroblast cell line, as a starting material for conversion. Using immunohistochemistry and qRT-PCR, we confirmed that this cell line was composed purely of mesodermal fibroblasts and was completely absent of neural progenitors, glia, or neural crest cells (Figs. S2*G* and S3 *A*–*H* and Tables S2 and S3). Similar to what was observed with hEFs, we could detect cells with a neuronal-like morphology a few days after transduction with the three conversion factors. The hiN cells derived from fetal lung fibroblasts stained positive for βIII-tubulin and MAP2 (Fig. 4*A*) and were converted with efficiencies comparable to hEFs: 8.0% ± 4.45% at day 12 ($n = 5$) and 12.3% ± 5.9% at day 20 ($n = 4$). Whole-cell patch–clamp recordings confirmed that HFL1-derived hiN cells exhibited properties of functional neurons (Fig. 4 *B* and *C* and Table S4). Resting membrane potential was approximately −62 mV, and TTX-sensitive action potentials were induced by depolarizing current in ∼80% of recorded cells (Fig. 4*B*). Depolarizing voltage steps induced in-

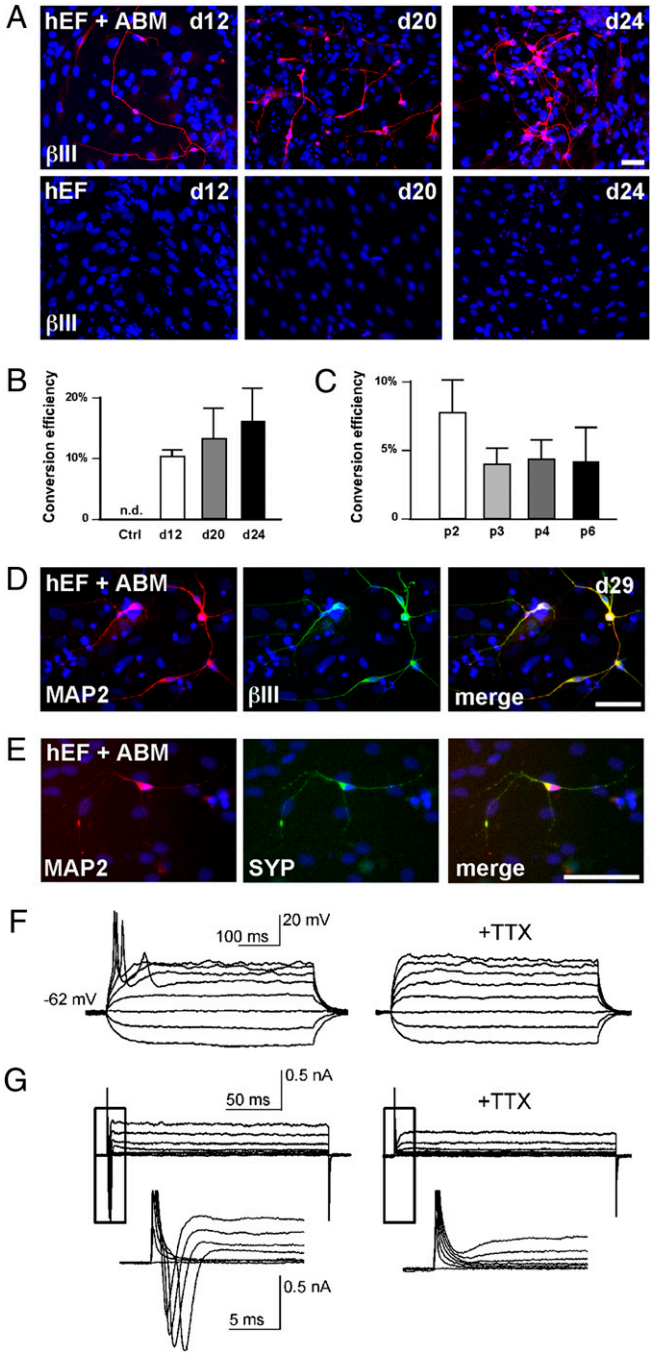

Fig. 2. Conversion of neurons from hEFs. (*A*) Neurons expressing βIII-tubulin (red) obtained by direct conversion of hEFs at 12, 20, and 24 d after Ascl1, Brn2, and Myt1l expression (ABM). Blue indicates DAPI counterstain. (*B* and *C*) Conversion efficiency estimation of hiN cell formation. ($n = 5$ for *B* and $n = 2$–4 for *C*.) (*D* and *E*) Immunocytochemical staining for MAP2 and synaptophysin (SYP) on the hEF-derived hiN cells. (*F*) Representative traces of membrane potential changes induced by current injection steps from −20 pA to +50 pA in 10-pA increments before (*Left*) and after (*Right*) TTX. (*G*) Representative traces of whole-cell currents induced by 10-mV depolarizing voltage steps from −60 mV to +10 mV before (*Left*; with inward Na^+ current) and after (*Right*; blocked Na^+ current) TTX. *Insets* show respective traces on an expanded scale. Bars represent average conversion efficiency from three to six separate experiments ± SD. (Scale bars: *A*, 50 μm; *D* and *E*, 100 μm.)

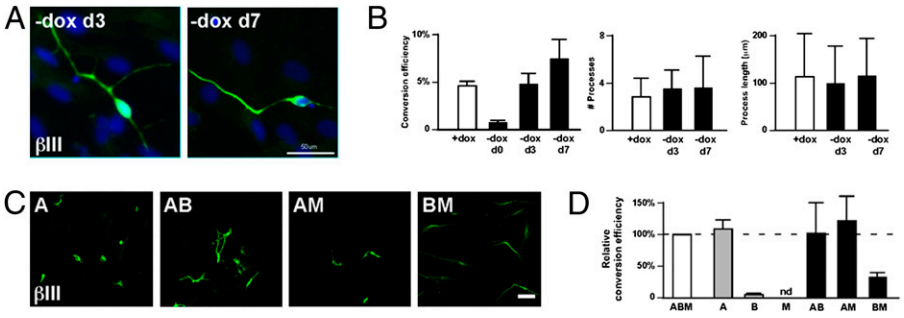

Fig. 3. Requirements for hiN conversion. (*A* and *B*) Removal of doxycycline at day 7 resulted in neurons expressing βIII (green) being formed with same efficiency and without affecting the morphological complexity of the resulting hiN cells ($n = 37$ for d3, $n = 68$ for d7, $n = 91$ for d0). (*C*) hiN cells expressing βIII-tubulin (green) obtained by conversion of hEFs in the presence of different combinations of Ascl1, Brn2, and Myt1l (ABM, A, B, M, AB, AM, and BM). (*D*) Conversion efficiency estimation of hiN cell formation using different combinations of conversion factors. Bars represent average conversion efficiency from three to six separate experiments ± SD.

ward currents (blocked by TTX) and outward currents. Several cells exhibited trains of action potentials in response to depolarizing current injection (Fig. 4*C*). Together, our data demonstrate that the hiN cells are derived from fibroblasts and provide evidence against the possibility that they originated from neural crest or other contaminating cell populations.

We next explored whether postnatal human fibroblasts could be directly converted to neurons. We used human foreskin fibroblasts (hFFs), a readily available postnatal source of cells that can be sufficiently expanded and is already used in clinical applications (13). The homogenous fibroblastic properties and absence of neural progenitors, neural crest cells, and glia was confirmed for hFFs (Figs. S1, S2*G*, and S3 and Tables S2 and S3). Similar to embryonic fibroblasts, the postnatal fibroblasts transduced with Ascl1, Brn2, and Myt1l gave rise to cells with a neuron-like morphology. When analyzed after 12 and 20 d, converted cells expressed MAP2 and βIII-tubulin with clear neuronal morphology (Fig. 5*A*). The conversion efficiency was slightly lower when using postnatal fibroblasts compared with embryonic cells as starting material: 4.3% ± 1.1% at day 12 ($n = 3$). Whole-cell patch–clamp recordings demonstrated that, 30 d after conversion, hFF-derived iN cells had a resting membrane potential of approximately −41 mV and exhibited electrophysiological properties characteristic of neurons (Table S4). Cells fired mature action potentials in response to depolarizing current injection, and depolarizing voltage steps induced large inward currents and outward currents (Fig. 5*B*). At 36 d after transduction, several cells exhibited TTX-sensitive trains of action potentials, indicating that the neurons matured over time (Fig. 5*C*).

When investigating the neurotransmitter phenotype of the converted neurons, we found that, similar to what has been reported for mouse iN cells (10), neurons of both excitatory glutamatergic and inhibitory GABAergic phenotypes were present in the cultures (Fig. 6 *A* and *B*). Also in agreement with the mouse iN cell phenotype, we could not detect any significant number of cholinergic, serotonergic, or dopaminergic neurons when screened for using immunocytochemistry for choline acetyltransferase, 5-hydroxytryptamine, and tyrosine hydroxylase (TH), respectively.

We next explored the possibility of directing the hiN cells into a specific neuronal subtype. We chose dopaminergic neurons, which would be of great interest from a clinical perspective because of their role in motor function and involvement in the pathogenesis of Parkinson's disease. To test whether expression of key transcription factors expressed during dopamine neuron development is sufficient to direct the hiN cells into a dopaminergic phenotype, we selected 10 genes involved in midbrain patterning and specification of dopamine neurons (*En1, Foxa2, Gli1, Lmx1a, Lmx1b, Msx1, Nurr1, Otx2, Pax2,* and *Pax5*) (14–21) and cloned them into lentiviral vectors. A pool of lentiviruses, LentiDA, containing all 10 genes was subsequently produced and validated (Fig. S4). We then performed the three-factor conversion of hEFs in combination with LentiDA and screened for the appearance of dopaminergic neurons after 12, 20, and 24 d. We found that a small, but reproducible, proportion of the hiN cells converted in the presence of LentiDA started to express TH 24 d after conversion (<1% of hiN cells) (Fig. 6 *C* and *F*). This finding provided proof of principle that formation of iN cells with specific neuronal subtypes can be achieved by transcription factor-mediated fate instruction combined with the three conversion factors.

We next set out to determine the minimal requirement for dopaminergic neuron fate specification. We found that when only Lmx1a and FoxA2 were expressed together with the three conversion factors, TH-expressing cells with typical morphology of cultured dopaminergic neurons could be detected from converted hEFs in much higher numbers (Fig. 6 *D* and *F*). Using HFL1 cells as starting material, conversion combined with expression of Lmx1a and FoxA2 gave rise to an even higher number of TH-expressing neurons (Fig. 6 *E* and *F*). The addition of Lmx1a and FoxA2 did not affect the conversion rate (Fig. S4*C*) nor did FoxA2 and Lmx1a induce neuron-like cells in the absence of the

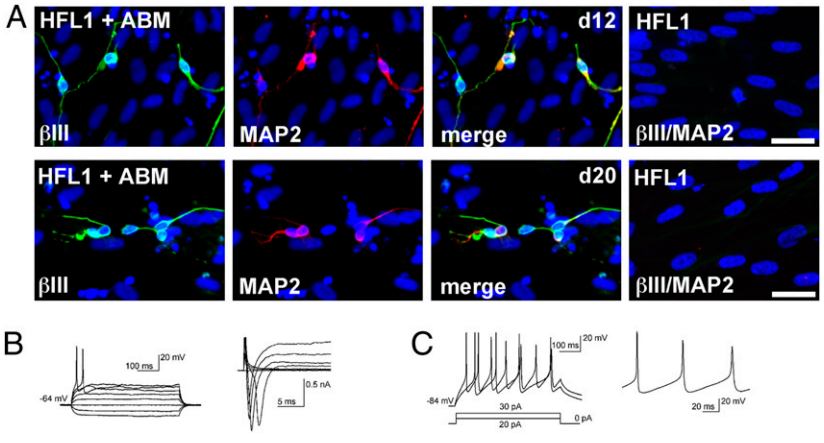

Fig. 4. Conversion of neurons from fetal lung fibroblasts. (*A*) Neurons expressing βIII-tubulin (green) and MAP2 (red) obtained by direct conversion of human fetal lung fibroblasts (HFL1) at 12 and 20 d after transduction with Ascl1, Brn2, and Myt1l (ABM). (*B*) Representative traces of membrane potential changes induced by current injection steps from −20 pA to +50 pA in 10-pA increments (*Left*) and representative traces of whole-cell currents induced by 10-mV depolarizing voltage steps from −60 mV to +10 mV (*Right*). (*C*) Representative traces of trains of action potentials induced by step injection of depolarizing current (*Right* shows traces on an expanded scale).

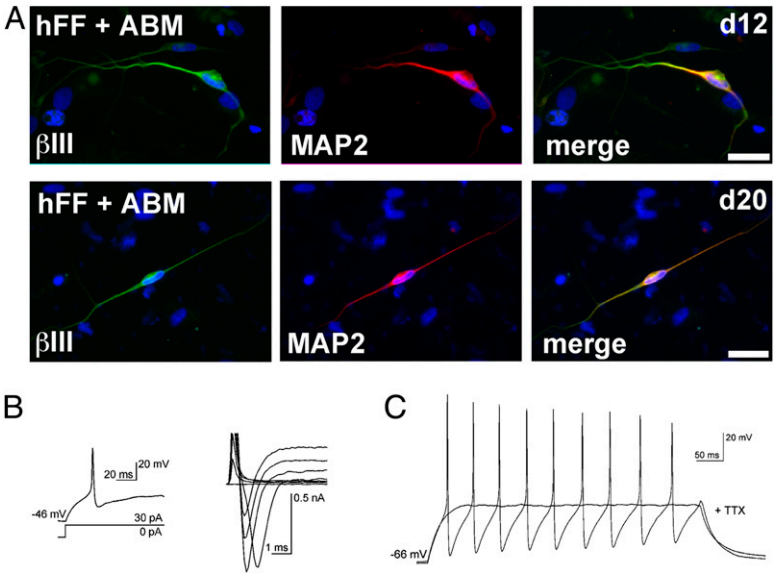

Fig. 5. Conversion of neurons from postnatal fibroblasts. (*A*) Neurons expressing βIII-tubulin (green) and MAP2 (red) obtained by direct conversion of hFFs at 12 and 20 d after transduction with Ascl1, Brn2, and Myt1l. (*B*) Representative trace of an action potential induced by depolarizing current injection (*Left*) and representative traces of whole-cell currents elicited in voltage–clamp mode by step depolarization (*Right*). (*C*) Representative trace of trains of action potentials induced by step injection of depolarizing current (20 pA) of hFF-derived iN cells, before and after TTX. (Scale bars: 50 μm.)

three conversion factors (Fig. S4*C*). The TH-expressing cells obtained from hEFs and HFL1 coexpressed βIII-tubulin (Fig. 6 *D* and *E*) but not the peripheral neuron marker peripherin (Fig. 6*G*). Aromatic L-amino acid decarboxylase (AADC), the second enzyme in dopamine synthesis and coexpression of Nurr1, an orphan nuclear receptor expressed by midbrain dopaminergic neurons, could also be detected in the TH-expressing cells (Fig. 6 *H* and *I*).

We found no TH neurons when hiN cells were generated with FoxA2 alone, whereas conversion in the presence of Lmx1a resulted in hiN cells expressing TH (Fig. 6*J*). However, none of the TH-expressing cells formed in the presence of Lmx1a alone coexpressed AADC (Fig. 6*K*). Whole-cell patch–clamp recordings demonstrated that hEF- and HFL1-derived iN cells converted in the presence of Lmx1a and FoxA2 were functional neurons (Table S5). At 28 d after conversion, action potentials could be induced by depolarizing current or occurred spontaneously (Fig. 6*K*). In current–clamp mode, a proportion of hEF-derived iN cells exhibited spontaneous action potentials, including pacemaker-like action potentials that were gradually blocked by adding TTX to the bath solution and rebound depolarizations resulting in action potentials after brief membrane hyperpolarizations (Fig. 6 *L* and *M*). Both spontaneous action potentials and rebound action potentials are characteristics compatible with midbrain dopamine neurons in vitro (22). Together, these data show that hiN cells generated from human fibroblasts via direct conversion can be further patterned into specific neuronal subtypes, exemplified here by the emergence of dopaminergic neurons after the addition of Lmx1a and FoxA2 during the conversion process.

Discussion

Our finding that human somatic cells, i.e., embryonic and postnatal fibroblasts, can be directly converted by using defined factors to functional neurons of a specific subtype is an important step toward developing iN cells for models of neurological disorders and brain repair.

A major concern when using primary fibroblasts for conversion is that contaminating neural progenitors, glia, or neural crest cells could be present in the starting material and selectively expanded when the embryonic fibroblasts are cultured in neural induction media and that these cells then serve as the cellular origin of iN cells (23). To exclude this possibility, we first confirmed that our hEF cultures were indeed composed of only collagen-producing cells. We also carefully screened the cultures with a panel of antibodies against neural progenitors, glia, and neural crest cells. After the first passage, a very small fraction of cells expressing p75 and/or *Sox10* could be detected, suggesting a small contaminating neural crest population. Given the extremely low proportion of neural crest cells in low-passage hEFs and the observation that multipassaged hEFs, which do not contain any neural crest contaminants, also efficiently converted into functional neurons, it is unlikely that the hiN cells are derived from neural crest cells. Subsequent conversions using HFL1 and hFFs, two commercially available human fibroblast cell lines that do not contain any contaminating cells, confirmed that the hiN cells were in fact derived from fibroblasts.

By expressing dopamine fate determinants during the conversion, we could demonstrate that additional fate specification of iN cells is possible. The proportion of hiN cells that developed into dopaminergic neurons when converted in the presence of Lmx1a and FoxA2 was ∼10%. Given that each cell needs to receive six viruses (A, B, M, Fuw, Lmx1a, and FoxA2) to differentiate into a dopamine neuron, this proportion is realistic and suggests that better delivery systems need to be developed in the future for more efficient conversion into dopamine neurons. Moreover, it will be interesting to explore the range of neuronal subtypes that can be formed via direct conversion by using combinations of other fate-determining genes or possibly by delivery of extrinsic factors.

An ultimate goal will be to use the hiN technology for disease modeling and cell therapy. As with iPS cells, iN cells circumvent the ethical concerns related to embryonic stem cell derivation and potential issues of allogenic rejection. In theory, the avoidance of reprogramming via a pluripotent state should reduce the risk of tumor formation after intracerebral grafting that is associated with the use of embryonic stem cells and iPS cells (24); thus, hiN cells may provide safer cells for transplantation in future applications. However, because the direct conversion does not go via a proliferative cell type, the number of neurons that can be obtained is limited by the accessible number of fibroblasts used as starting material for conversion. When using embryonic fibroblasts, this does not pose a serious limitation but could be limiting if generating patient-specific cells for disease modeling or autologous cell therapy.

Future studies should aim to increase the efficiency of hiN formation and the rate of dopaminergic neuron generation as well as to evaluate the converted dopaminergic neurons' ability to survive long term, reinnervate the denervated striatum, and ameliorate behavioral deficits after transplantation in rodent models of Parkinson's disease. Before clinical application of hiN cells can be considered, it will be critical to determine the optimal starting cell that can be obtained in sufficient numbers, to develop viral- and integration-free conversion systems, and to confirm the functionality and safety of hiN cells in vivo.

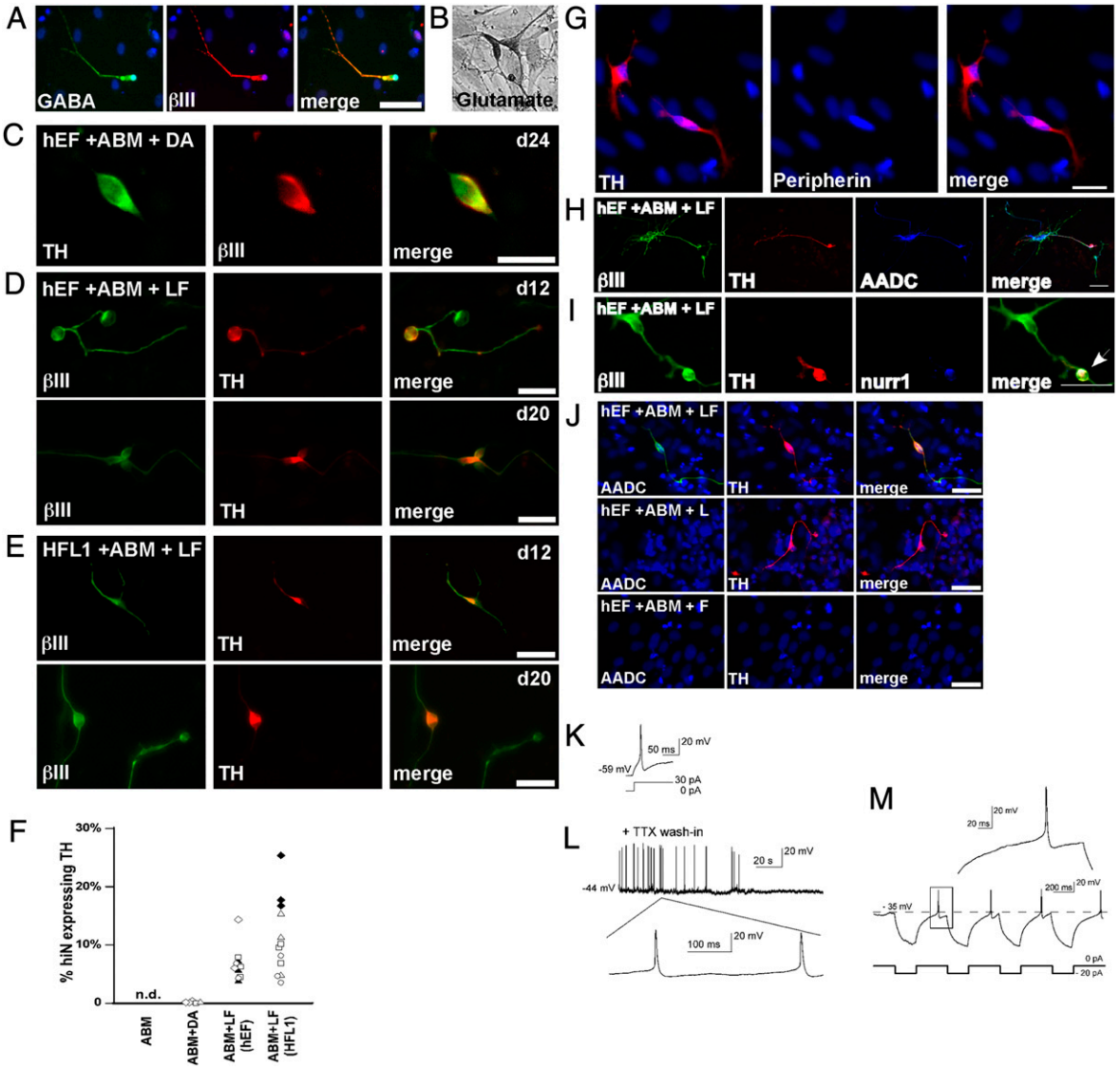

Fig. 6. Generation of dopamine neurons via direct conversion. (*A* and *B*) GABAergic and glutamatergic expressing hiN cells obtained by conversion with Ascl1, Brn2, and Myt1l. (*C* and *D*) hiN cells expressing TH (green) and βIII-tubulin (red) obtained by conversion of hEFs using Ascl1, Brn2, and Myt1l in combination with LentiDA, containing 10 genes involved in midbrain patterning and dopamine neuron differentiation (*C*) or in combination with Lmx1a and FoxA2 (LF) (*D*). (*E*) hiN cells expressing TH (green) and βIII-tubulin (red) obtained by conversion of HFL1 cells using Ascl1, Brn2, and Myt1l in combination with Lmx1a and Foxa2 (ABM + LF). (*F*) Quantification of dopaminergic neurons. Each symbol represents values obtained from separate biological replicates. Solid black symbols indicate data obtained when Lmx1a and FoxA2 were delivered 3 d after ABM; all other data points are from simultaneous delivery of all factors. (*G*) TH-expressing neurons (red) did not express peripherin (green). (*H* and *I*) hiN cells positive for TH (red) and βIII-tubulin (green) coexpress AADC (blue) and Nurr1 (blue; arrowhead). (*J*) TH (red) and AADC (green) expression in hiN cells obtained by conversion in the presence of Lmx1a and FoxA2 (LF; *Top*), Lmx1a alone (L; *Middle*), or FoxA2 alone (F; *Bottom*). (*K*) Example of an ABM + LF hEF iN cell exhibiting spontaneous, pacemaker-like action potentials that were gradually blocked by the addition of TTX to the bath solution. (*L*) Representative trace of an action potential induced by depolarizing current injection. (*M*) Example of an ABM + LF hEF iN cell exhibiting rebound depolarizations at the offset of brief membrane hyperpolarizations. *Insets* show respective traces on an expanded scale. (Scale bars: 50 μm.)

Methods

Tissue Sources and Cell Preparations. Fibroblasts were isolated from legally aborted fetuses aged 5.5–7 wk postconception, with approval of the Swedish National Board of Health and Welfare and the Lund/Malmö Ethics Committee (see Table S1 for details). Great care was taken to remove the head, vertebral column, dorsal root ganglia, and all inner organs to discard cells with a neurogenic potential. The remaining tissue was manually dissociated in 0.25% trypsin (Sigma), incubated at 37 °C to make a single-cell suspension, and then plated in T75 bottles. Cells were grown at 37 °C in 5% CO_2 in MEF medium, DMEM (Gibco) with 100 mg/mL penicillin/streptomycin (Sigma), 2 nM L-glutamine (Sigma), and 10% FBS (Biosera) until confluent. The cells were then dissociated with 0.25% trypsin, spun, and frozen in 50/50 DMEM/FBS with 10% DMSO (Sigma).

HFL1 (ATCC-CCL-153) and hFF (ATCC-CRL-2429) cells were obtained from the American Type Culture Collection, expanded in hEF medium until confluent, and then frozen.

For neuronal conversion, fibroblasts were plated in MEF medium at a density of 10,000 cells per cm^2 in tissue culture plates (Nunc) coated with 0.1% gelatin. Neuronal conversion was performed as previously described (10) with N3 medium, which is composed of DMEM/F12, 25 g/mL insulin, 50 g/mL transferrin, 30 nM sodium selenite, 20 nM progesterone (Sigma), 100 nM putrescine (Sigma), and penicillin/streptomycin.

Viral Vectors. Doxycycline-regulated lentiviral vectors expressing mouse cDNAs for Ascl1, Brn2, and Myt1l have been described elsewhere (10). The doxycycline-regulated system includes a separate lentiviral vector expressing

a Tet-On transactivator (FUW.rtTA-SM2; Addgene) that was always co-transduced in the conversion experiments.

Lentiviral vectors expressing mouse ORFs for En1, Foxa2, Gli1, Lmx1a, Lmx1b, Msx1, Nurr1, Otx2, Pax2, and Pax5 were generated by replacing GFP in a third-generation lentiviral vector containing a nonregulated, ubiquitous phosphoglycerate kinase promoter with the various ORFs (25). Plasmids containing the different cDNAs were purchased from Genecopoeia and subsequently verified by sequencing. Third-generation lentiviral vectors were produced as previously described (26) and titrated by quantitative PCR analysis (27). The titers of the vectors used in this study were in the range of 5×10^8 to 2×10^9 transducing units per mL. A multiplicity of infection of 2–3 was used for hEF and HFL1 cells.

Immunocytochemistry. Cells were fixed in 4% paraformaldehyde and preincubated for 30–60 min in blocking solution (5% normal serum and 0.25% Triton-X in 0.1 M potassium-buffered PBS). The primary antibodies (Table S6) were diluted in the blocking solution and applied overnight at 4 °C. Fluorophore-conjugated secondary antibodies (Molecular Probes or Jackson Laboratories) were diluted in blocking solution and applied for 2 h followed by three rinses in potassium PBS.

Quantifications and Efficiency Calculation. ***Efficiency determination.*** The total number of βIII-positive/MAP2-positive cells with a neuronal morphology and absence of fibroblast-like morphology were counted in 36 randomly selected 20× visual fields. This sampling was repeated three times, and the average number was used to calculate the mean number of positive cells per visual field. From this value, the total number of neurons per dish was estimated and, by following the method used by Vierbuchen et al. (10), the conversion efficiency was determined by dividing the number of neurons formed by the number of fibroblasts plated before infection.

TH quantifications. The total number of neurons per well was determined as described above. The total number of TH-expressing neurons per well was determined in the same manner or, when the number of TH neurons was low (<100), also by counting all of the TH-positive cells in the well.

Quantification of process length and number. Digital images were obtained with a Leica microscope and analyzed with Canvas IX. Total process length was determined by tracing each individual neuron, and the number of end processes was counted manually for the same cells.

Quantitative RT-PCR (qRT-PCR). Total RNA was isolated by using the RNeasy Micro Kit (Qiagen) according to the supplier's recommendations. For each sample, 1–4 mg of RNA was used for reverse transcription performed with random primers and SuperScriptIII (Invitrogen). SYBR green quantitative real-time PCR was performed with LightCycler 480 SYBR Green I Master (Roche) in a two-step cycling protocol. Data were quantified by using the $\Delta\Delta C_T$ method and averaged upon normalization to GAPDH and β-actin expression. The specificity was confirmed by analyzing the dissociation curve and by validation in human embryonic tissue. Primer sequences are shown in Table S7.

Electrophysiology. Cells with neuronal morphology (round cell body and processes resembling neurites) were selected for whole-cell patch–clamp recordings at the indicated time points. Cells plated on coverslips were placed in a submerged recording chamber and constantly perfused with gassed bath solution (95% O_2/5% CO_2, pH 7.2–7.4, 295–300 mOsm, 32–34 °C) containing 119 mM NaCl, 2.5 mM KCl, 1.3 mM $MgSO_4$, 2.5 mM $CaCl_2$, 26 mM $NaHCO_3$, 1.25 mM NaH_2PO_4, and 25 mM glucose. Cells for recording were visualized under infrared light with differential interference contrast using an Olympus upright microscope equipped with a digital camera and a 40× water-immersion lens. Recording pipettes were filled with solution (pH 7.2–7.4, 295–300 mOsm) containing 122.5 mM potassium gluconate, 12.5 mM KCl, 10.0 mM KOH-Hepes, 0.2 mM KOH-EGTA, 2.0 mM MgATP, 0.3 mM Na_3-GTP, and 8.0 mM NaCl, resulting in pipette resistances of 3–4 Ω. Biocytin (0.5%; Sigma-Aldrich) was freshly dissolved in the pipette solution before recordings for post hoc identification of recorded cells. Resting membrane potential was estimated in current–clamp mode immediately after breaking the membrane and establishing whole-cell configuration. For measurements of action potentials and voltage responses, cells were current–clamped between −55 mV and −85 mV (depending on resting membrane potential), and 500-ms hyperpolarizing and depolarizing current steps were delivered in 10-pA increments through the whole-cell pipette. Spontaneous action potentials were measured in current–clamp mode (0 pA), and rebound action potentials were induced by brief injections of hyperpolarizing current (−20 pA). For measurements of whole-cell currents, cells were voltage–clamped between −60 mV and −70 mV, and 200-ms voltage steps were delivered in 10-mV increments. Voltage-gated sodium channels were blocked with 1 μM TTX (Tocris). Data were filtered at 2.9 kHz and sampled at 10 kHz with an EPC9 patch–clamp amplifier (HEKA Elektronik). Capacitance was compensated. Input resistance was measured at a holding potential of −60 mV by delivering −5-mV test pulses. Action potential amplitude was measured from the threshold to the peak voltage deflection, whereas half-width was measured as the duration of the action potential at half maximum amplitude. After-hyperpolarization amplitude was measured as the difference between the resting membrane potential and the maximum hyperpolarization after the action potential, whereas duration was measured as the time between the start and end of the hyperpolarization.

ACKNOWLEDGMENTS. We thank C. Isacsson, U. Jarl, B. Mattsson, I. Nilsson, and A.-K. Olden for technical assistance; M. Wernig, D. Trono, and L. Naldini for providing lentiviral vector plasmids; Z. Kokaia and J. Reimer for collaborative work on the human tissue collection; M. Kokaia for advice on electrophysiology; and K. Nihlberg and A. Malmström for advice on fibroblast culturing. This work was supported by Grant 22943 from the European Community's 7th Framework Programme through NeuroStemCell; Swedish Research Council Grants K2007-62X-20391-01-4 (to M.P.), K2007-62P-20390-01-4 (to M.P.), and K2010-80P-21583-01-4 (to J.J.); Bagadilico Grant 349-2007-8626 (to M.P.); StemTherapy (O.L.); the Crafoord Foundation (M.P.); the Swedish Parkinson Foundation (M.P.); the Jeansson Foundation (M.P.); Lundbeck Foundation Grant R44-A3856 (A.K.); the M. Lundqvist Foundation (J.J.); the Knut and Alice Wallenberg Foundation (A.B.); and the Human Frontiers Science Program (A.D.).

1. Takahashi K, et al. (2007) Induction of pluripotent stem cells from adult human fibroblasts by defined factors. *Cell* 131:861–872.
2. Takahashi K, Yamanaka S (2006) Induction of pluripotent stem cells from mouse embryonic and adult fibroblast cultures by defined factors. *Cell* 126:663–676.
3. Yu J, et al. (2007) Induced pluripotent stem cell lines derived from human somatic cells. *Science* 318:1917–1920.
4. Ebert AD, et al. (2009) Induced pluripotent stem cells from a spinal muscular atrophy patient. *Nature* 457:277–280.
5. Park IH, et al. (2008) Reprogramming of human somatic cells to pluripotency with defined factors. *Nature* 451:141–146.
6. Forsberg M, et al. (2010) Efficient reprogramming of adult neural stem cells to monocytes by ectopic expression of a single gene. *Proc Natl Acad Sci USA* 107:14657–14661.
7. Ieda M, et al. (2010) Direct reprogramming of fibroblasts into functional cardiomyocytes by defined factors. *Cell* 142:375–386.
8. Takeuchi JK, Bruneau BG (2009) Directed transdifferentiation of mouse mesoderm to heart tissue by defined factors. *Nature* 459:708–711.
9. Zhou Q, Brown J, Kanarek A, Rajagopal J, Melton DA (2008) In vivo reprogramming of adult pancreatic exocrine cells to β-cells. *Nature* 455:627–632.
10. Vierbuchen T, et al. (2010) Direct conversion of fibroblasts to functional neurons by defined factors. *Nature* 463:1035–1041.
11. Wernig M, et al. (2002) Tau EGFP embryonic stem cells: An efficient tool for neuronal lineage selection and transplantation. *J Neurosci Res* 69:918–924.
12. Breul SD, et al. (1980) Control of collagen production by human diploid lung fibroblasts. *J Biol Chem* 255:5250–5260.
13. Hovatta O, et al. (2003) A culture system using human foreskin fibroblasts as feeder cells allows production of human embryonic stem cells. *Hum Reprod* 18:1404–1409.
14. Acampora D, et al. (1995) Forebrain and midbrain regions are deleted in *Otx2*$^{-/-}$ mutants due to a defective anterior neuroectoderm specification during gastrulation. *Development* 121:3279–3290.
15. Andersson E, et al. (2006) Identification of intrinsic determinants of midbrain dopamine neurons. *Cell* 124:393–405.
16. Ferri AL, et al. (2007) Foxa1 and Foxa2 regulate multiple phases of midbrain dopaminergic neuron development in a dosage-dependent manner. *Development* 134:2761–2769.
17. Simon HH, Saueressig H, Wurst W, Goulding MD, O'Leary DD (2001) Fate of midbrain dopaminergic neurons controlled by the engrailed genes. *J Neurosci* 21:3126–3134.
18. Smidt MP, et al. (2000) A second independent pathway for development of mesencephalic dopaminergic neurons requires Lmx1b. *Nat Neurosci* 3:337–341.
19. Urbánek P, Fetka I, Meisler MH, Busslinger M (1997) Cooperation of *Pax2* and *Pax5* in midbrain and cerebellum development. *Proc Natl Acad Sci USA* 94:5703–5708.
20. Zervas M, Millet S, Ahn S, Joyner AL (2004) Cell behaviors and genetic lineages of the mesencephalon and rhombomere 1. *Neuron* 43:345–357.
21. Zetterström RH, et al. (1997) Dopamine neuron agenesis in Nurr1-deficient mice. *Science* 276:248–250.
22. Grace AA, Onn SP (1989) Morphology and electrophysiological properties of immunocytochemically identified rat dopamine neurons recorded in vitro. *J Neurosci* 9:3463–3481.
23. Sareen D, Svendsen CN (2010) Stem cell biologists sure play a mean pinball. *Nat Biotechnol* 28:333–335.
24. Miura K, et al. (2009) Variation in the safety of induced pluripotent stem cell lines. *Nat Biotechnol* 27:743–745.
25. Brown BD, et al. (2007) Endogenous microRNA can be broadly exploited to regulate transgene expression according to tissue, lineage and differentiation state. *Nat Biotechnol* 25:1457–1467.
26. Zufferey R, Nagy D, Mandel RJ, Naldini L, Trono D (1997) Multiply attenuated lentiviral vector achieves efficient gene delivery in vivo. *Nat Biotechnol* 15:871–875.
27. Georgievska B, et al. (2004) Regulated delivery of glial cell line-derived neurotrophic factor into rat striatum, using a tetracycline-dependent lentiviral vector. *Hum Gene Ther* 15:934–944.